A quasiclassical approach to strongly correlated quantum dots in intense magnetic fields

2005 J. Phys.: Condens. Matter 17 3851

(http://iopscience.iop.org/0953-8984/17/25/012)

INSTITUTE OF PHYSICS PUBLISHING JOURNAL OF PHYSICS: CONDENSED MATTER

J. Phys.: Condens. Matter **17** (2005) 3851–3864 doi:10.1088/0953-8984/17/25/012

A quasiclassical approach to strongly correlated quantum dots in intense magnetic fields

A Matulis and E Anisimovas

Semiconductor Physics Institute, Goštauto 11, LT-01108 Vilnius, Lithuania

Received 17 March 2005, in final form 2 May 2005
Published 10 June 2005
Online at stacks.iop.org/JPhysCM/17/3851

Abstract

We present a general quasiclassical description of parabolic many-electron quantum dots in the limit of high magnetic fields. The key points of our approach are the transition to a rotating frame of reference, in order to decouple rotational and vibrational modes, as well as the recognition and inclusion of the role of potential anisotropy felt by the vibrational modes. We are able to obtain the complete wavefunction of quantum dots containing any number of electrons in the Gaussian form, and present results concerning inter-particle correlation and deformation of large quantum dots.

1. Introduction

There persists continuous interest in the electronic properties of quantum dots that confine a small number N of electrons to a volume of nanometric extensions [1–4]. Among the most stimulating topics of theoretical research performed on quantum dots [3] is the strong electron–electron correlation which, further enhanced by application of a magnetic field, induces the formation of Wigner crystallites [5, 6].

These many-body phenomena are hard to calculate since the separation of variables making use of a single-particle approach is not possible. To a certain extent, the many-body problem can be managed by mapping it onto an equivalent problem of independent particles moving in an effective potential as in the density functional [4], Hartree or Hartree–Fock approaches. However, these techniques are of limited use in the realm of strong inter-particle correlations.

Equally restrictive is the use of the exact diagonalizations [5, 7, 8]. In this approach one fully accounts for the Coulomb interactions but the ensuing numerical work becomes daunting when the number of particles exceeds a few. Significant results have been obtained for a small number of electrons or at very high magnetic fields [9] where the approximation of the lowest Landau level is applicable.

The composite fermion model [10–12] evolved from the suggestion of replacing bare electrons by quasiparticles of another type, the composite fermions [13, 14], formed by dressing the electrons with an even number of magnetic flux quanta. However, it turned out [15] that this method also becomes rather inaccurate in the regime of very high magnetic fields where one

expects the Wigner crystal to be formed. The authors of [15] found that the rotating electron molecule [16] approach becomes superior.

In our earlier work [17, 18] we have shown that the Wigner crystallization as well as the ground state multiplicity transitions may be successfully addressed employing a quasiclassical expansion in powers of $1/B$. This line of development has led us to an analytical expression for the many-electron wavefunction for symmetric configurations when all the electrons crystallize into a single ring.

The purpose of the present paper is to develop a comprehensive quasiclassical theory based on the aforementioned $1/B$ expansion and applicable to quantum dots containing an arbitrary number of electrons. This theory may be regarded as a quantum mechanical generalization of the classical treatment due to Bedanov and Peeters [19]. Classical Wigner crystallites have already been addressed experimentally [20]. On the other hand, the frontiers of research on quantum mechanical phenomena have advanced to embrace the possibility of imaging the electronic wavefunctions [21]. In this context, the theoretical investigation of electronic wavefunctions and complex electron configurations in quantum dots is gaining practical importance. Knowledge of correlation functions may also be relevant with the prospect of dynamical wavefunction control experiments, already carried out on natural atoms [22].

We consider quantum dots with a circularly symmetric isotropic parabolic confining potential. However, due to the discreteness of charge the actual symmetry of the dots is lower and there arises a local anisotropy of the electron–electron interaction which it is necessary to take into account. The influence of this anisotropy on the shape of the wavefunction does not disappear even in the limit of extreme magnetic fields. Indeed, we find important corrections to the previous results [18] which overlooked the potential anisotropy. The proper recognition of the anisotropy felt by the collective electronic modes is influencing the conditions for emergence of inter-shell rotations.

The quasiclassical theory is presented in the four subsections of section 2. In the following section 3 we introduce the quasiclassical correlation functions and use them to describe the structural properties of quantum dots. Two topics (the calculation of the potential expansion and the discussion of the anisotropy effects) are discussed in the appendices.

2. Quasiclassical theory

We consider an arbitrary number N of two-dimensional electrons of effective mass m^* moving in an external confining potential $V_c = \frac{1}{2}m^*\omega_0^2 r^2$ and a perpendicular magnetic field $\boldsymbol{B}$ described in terms of its symmetric gauge vector potential $\boldsymbol{A} = \frac{1}{2}[\boldsymbol{B} \times \boldsymbol{r}]$. It is convenient to work in the natural dimensionless units defined by using the oscillator length $l_0 = \sqrt{\hbar/m\omega_0}$ as the unit of length and the confinement energy $\hbar\omega_0$ as the energy unit. Correspondingly, the dimensionless magnetic field is measured in units $\Phi_0/2\pi l_0^2$, with $\Phi_0 = hc/e$ being the magnetic flux quantum. The relative strength of the Coulomb coupling between electrons is then given by the dimensionless coupling constant $\lambda = l_0/a_B^*$ equal to the ratio of the confinement length to the effective Bohr radius $a_B^* = \epsilon\hbar^2/m^*e^2$. Here ϵ denotes the dielectric constant of the medium.

2.1. Lagrangian formalism

Like in the previous—restricted to systems containing less than five electrons—treatment [18] we face the necessity of switching to a rotating (Eckart) frame of [23, 24] in order to deal with the compensation of the strong magnetic field by a high value of the ground state angular momentum M. The change of the reference frame is easily performed in the Lagrangian

formalism starting with the laboratory frame Lagrangian $L = L_{\rm mag} - V$ which we explicitly split into two parts. The first term

$$L_{\rm mag} = \tfrac{1}{2}\sum_{n=1}^{N}\{\dot{\boldsymbol{r}}_n^2 - [\boldsymbol{B}\times\boldsymbol{r}_n]\dot{\boldsymbol{r}}_n\} \tag{1}$$

is the sum of free-electron Lagrangians in a magnetic field, and the remaining part

$$V = \frac{1}{2}\sum_{n=1}^{N}\boldsymbol{r}_n^2 + \sum_{\substack{n,m=1\\ n>m}}^{N}\frac{\lambda}{|\boldsymbol{r}_n - \boldsymbol{r}_m|} \tag{2}$$

is the total (the confinement plus the Coulomb interaction) potential energy.

We begin our progress towards the quasiclassical theory from the extreme limit of an infinite magnetic field. In these circumstances the kinetic energy is completely frozen out, and the electrons crystallize into a finite-size Wigner molecule. We determine the ground state configuration of an N-electron system by using a numerical Monte Carlo procedure [19] to minimize the potential energy (2), and thereby obtain a set of vectors $\boldsymbol{a}_n$ giving the equilibrium positions of the electrons. Generally, the equilibrium configuration consists of a number of deformed concentric rings.

Paralleling the development in the special single-ring case [18] we introduce local coordinate systems for the individual electrons. Thus, the coordinate x_n measures the deviation of the nth electron from its equilibrium position in the radial direction (i.e. along $\boldsymbol{a}_n$), and y_n anticlockwise in the azimuthal direction. We find it convenient to collect the electron coordinates into two N-component vectors

$$\boldsymbol{x} = \{x_1, x_2, \ldots, x_N\}, \qquad \boldsymbol{y} = \{y_1, y_2, \ldots, y_N\}, \tag{3}$$

and introduce the corresponding vector

$$\boldsymbol{a} = \{a_1, a_2, \ldots, a_N\} \tag{4}$$

containing the equilibrium radii of the electrons. Using the above definitions we obtain the rotating frame Lagrangian in a concise N-vector notation:

$$L_{\rm mag} = \frac{I}{2}\left(\omega^2 - \frac{B^2}{4}\right) + \frac{1}{2}(\dot{\boldsymbol{x}}^{\rm T}\dot{\boldsymbol{x}} + \dot{\boldsymbol{y}}^{\rm T}\dot{\boldsymbol{y}}) + \omega(\boldsymbol{x}^{\rm T}\dot{\boldsymbol{y}} - \dot{\boldsymbol{x}}^{\rm T}\boldsymbol{y}), \tag{5a}$$

$$I = I_0 + 2\boldsymbol{a}^{\rm T}\boldsymbol{x} + \boldsymbol{x}^{\rm T}\boldsymbol{x} + \boldsymbol{y}^{\rm T}\boldsymbol{y}, \tag{5b}$$

$$I_0 = \boldsymbol{a}^{\rm T}\boldsymbol{a} = a^2. \tag{5c}$$

Here, $\omega = \dot{\chi} - B/2$ and the superscript T is used to denote transposed vectors and matrices.

The introduction of the frame rotation angle χ as an additional degree of freedom is balanced by a constraint [18]

$$\boldsymbol{a}^{\rm T}\boldsymbol{y} = 0, \tag{6}$$

expressing the elimination of the total angular momentum in the Eckart frame.

We use the harmonic approximation for the potential energy V. That is, we expand V in the Taylor series in the vicinity of the equilibrium configuration and take into account only the second-order term. This term is a quadratic form which in the N-vector notation reads

$$V_2 = \tfrac{1}{2}\{\boldsymbol{x}^{\rm T}\mathcal{A}\boldsymbol{x} + \boldsymbol{y}^{\rm T}\mathcal{D}\boldsymbol{y} + \boldsymbol{x}^{\rm T}\mathcal{B}\boldsymbol{y} + \boldsymbol{y}^{\rm T}\mathcal{B}^{\rm T}\boldsymbol{x}\}. \tag{7}$$

The matrices $\mathcal{A}$, $\mathcal{B}$, and $\mathcal{D}$ are computed numerically with the aid of expressions given in appendix A.

In order to account for the condition (6) in an easy way we introduce a new set of collective coordinates in place of $\boldsymbol{y}$ by means of a transformation

$$\boldsymbol{y} = \mathcal{Q}\boldsymbol{v}, \qquad \boldsymbol{v} = \{v_0, v_1, \ldots, v_{N-1}\}. \tag{8}$$

The transformation matrix $\mathcal{Q}$ is constructed as follows. The first column of $\mathcal{Q}$ is taken equal to the normalized vector (4), that is,

$$\mathcal{Q}_{n,0} = (\boldsymbol{Q}_0)_n, \qquad \boldsymbol{Q}_0 = \frac{\boldsymbol{a}}{|\boldsymbol{a}|}, \tag{9}$$

and all the remaining columns are chosen orthogonal to $\boldsymbol{Q}_0$ and to each other. Thus, the matrix $\mathcal{Q}$ is a real orthogonal matrix

$$\mathcal{Q}^{\mathrm{T}}\mathcal{Q} = \mathcal{Q}\mathcal{Q}^{\mathrm{T}} = \mathcal{I}, \tag{10}$$

and in the new azimuthal coordinates the constraint (6) transforms to the condition $v_0 = 0$, that is, the mode v_0 has to be excluded.

We further use the same transformation matrix $\mathcal{Q}$ to introduce the collective radial coordinates

$$\boldsymbol{x} = \mathcal{Q}\boldsymbol{u}. \tag{11}$$

The mode u_0 is the so-called *breathing* mode. In this mode, the radial displacements of the individual electrons are proportional to their equilibrium radii a_n.

As discussed in appendix A, by virtue of the collective coordinates $\boldsymbol{u}$ and $\boldsymbol{v}$ the breathing and rotational modes separate from the remaining $2N-2$ vibrational modes. Thus, we may explicitly isolate these special modes and rewrite the matrices defining the potential quadratic form V_2 as

$$\mathcal{Q}^{\mathrm{T}}\mathcal{A}\mathcal{Q} = \begin{pmatrix} 3 & 0 \\ 0 & \tilde{\mathcal{A}} \end{pmatrix}, \qquad \mathcal{Q}^{\mathrm{T}}\mathcal{D}\mathcal{Q} = \begin{pmatrix} 0 & 0 \\ 0 & \tilde{\mathcal{D}} \end{pmatrix}, \qquad \mathcal{Q}^{\mathrm{T}}\mathcal{B}\mathcal{Q} = \begin{pmatrix} 0 & 0 \\ 0 & \tilde{\mathcal{B}} \end{pmatrix}. \tag{12}$$

Here we took into account the fact that the frequencies of the breathing and rotational modes equal $\sqrt{3}$ and 0, respectively, for any number of electrons.

Besides reduced $(N-1)\times(N-1)$ matrices (denoted by tildes) we also introduce reduced vectors with $(N-1)$ components:

$$\tilde{\boldsymbol{u}} = \{v_1, \ldots, v_{N-1}\}, \qquad \tilde{\boldsymbol{v}} = \{v_1, \ldots, v_{N-1}\}. \tag{13}$$

In these new variables the two constituent parts of the Lagrangian become

$$L_{\mathrm{mag}} = \frac{I}{2}\left(\omega^2 - \frac{B^2}{4}\right) + \frac{1}{2}(\dot{u}_0^2 + \dot{\tilde{\boldsymbol{u}}}^{\mathrm{T}}\dot{\tilde{\boldsymbol{u}}} + \dot{\tilde{\boldsymbol{v}}}^{\mathrm{T}}\dot{\tilde{\boldsymbol{v}}}) + \omega(\tilde{\boldsymbol{u}}^{\mathrm{T}}\dot{\tilde{\boldsymbol{v}}} - \dot{\tilde{\boldsymbol{u}}}^{\mathrm{T}}\tilde{\boldsymbol{v}}), \tag{14a}$$

$$I = (|\boldsymbol{a}| + u_0)^2 + \tilde{\boldsymbol{u}}^{\mathrm{T}}\tilde{\boldsymbol{u}} + \tilde{\boldsymbol{v}}^{\mathrm{T}}\tilde{\boldsymbol{v}}, \tag{14b}$$

and

$$V_2 = \tfrac{1}{2}\{3u_0^2 + \tilde{\boldsymbol{u}}^{\mathrm{T}}\tilde{\mathcal{A}}\tilde{\boldsymbol{u}} + \tilde{\boldsymbol{v}}^{\mathrm{T}}\tilde{\mathcal{D}}\tilde{\boldsymbol{v}} + \tilde{\boldsymbol{u}}^{\mathrm{T}}\tilde{\mathcal{B}}\tilde{\boldsymbol{v}} + \tilde{\boldsymbol{v}}^{\mathrm{T}}\tilde{\mathcal{B}}^{\mathrm{T}}\tilde{\boldsymbol{u}}\}. \tag{14c}$$

2.2. Hamiltonian

The Hamiltonian is obtained from the Lagrangian (14*a*) in the standard way. We first define the generalized momenta

$$\begin{aligned} M &= \frac{\partial}{\partial\dot{\chi}}L_{\mathrm{mag}} = \omega I + \tilde{\boldsymbol{u}}^{\mathrm{T}}\dot{\tilde{\boldsymbol{v}}} - \dot{\tilde{\boldsymbol{u}}}^{\mathrm{T}}\tilde{\boldsymbol{v}}, \\ U_0 &= \frac{\partial}{\partial\dot{u}_0}L_{\mathrm{mag}} = \dot{u}_0 \end{aligned} \tag{15}$$

and for $1 \leqslant n \leqslant N-1$

$$\begin{aligned} \tilde{\boldsymbol{U}} &= \frac{\partial}{\partial \dot{\tilde{\boldsymbol{u}}}} L_{\mathrm{mag}} = \dot{\tilde{\boldsymbol{u}}} - \omega \tilde{\boldsymbol{v}}_n, \\ \tilde{\boldsymbol{V}} &= \frac{\partial}{\partial \dot{\tilde{\boldsymbol{v}}}} L_{\mathrm{mag}} = \dot{\tilde{\boldsymbol{v}}} + \omega \tilde{\boldsymbol{u}}. \end{aligned} \tag{16}$$

Expressing the velocities in terms of the generalized momenta from equations (15), (16) and substituting them into

$$H_{\mathrm{mag}} = M\dot{\chi} + U_0 \dot{u}_0 + \tilde{\boldsymbol{U}}\dot{\tilde{\boldsymbol{u}}} + \tilde{\boldsymbol{V}}\dot{\tilde{\boldsymbol{v}}} - L_{\mathrm{mag}}, \tag{17}$$

after some algebraic manipulations we arrive at

$$H = \frac{1}{2I_b}\left(M + \frac{BI_b}{2} - J\right)^2 + \frac{1}{2}\left\{U_0^2 + \left(\tilde{U} - \frac{B}{2}\tilde{\boldsymbol{v}}\right)^2 + \left(\tilde{\boldsymbol{V}} + \frac{B}{2}\tilde{\boldsymbol{u}}\right)^2\right\} + V_2. \tag{18}$$

Here, the quantity $J = \tilde{\boldsymbol{u}}^{\mathrm{T}}\tilde{\boldsymbol{V}} - \tilde{\boldsymbol{U}}^{\mathrm{T}}\tilde{\boldsymbol{v}}$ expresses the sum of local electronic angular momenta, and $I_b = (|\boldsymbol{a}| + u_0)^2$.

The first term of the Hamiltonian apparently still poses a considerable challenge as it includes coupling between different modes. Nevertheless, analysing the nature and relative magnitudes of the terms inside the parentheses we find that the following approximation can be made:

$$\frac{1}{2I_b}\left(M + \frac{B|\boldsymbol{a}|^2}{2} + B|\boldsymbol{a}|u_0 + \frac{Bu_0^2}{2} - J\right)^2 \to \frac{B^2u_0^2}{2}. \tag{19}$$

Briefly, the local angular momentum operator J may be omitted since it is of order 1 and symmetric in coordinates $\tilde{\boldsymbol{u}}$, so that its action is not enhanced by anisotropy, and the same applies to the term $\frac{1}{2}Bu_0^2$. The terms M and $\frac{1}{2}B|\boldsymbol{a}|^2$ are both large ($\sim B$); however, in the ground state the system chooses its angular momentum so as to maximally compensate the magnetic field term. Only due to the integer quantization of M is there a remainder of the order of unity, which also may be safely neglected.

Thus, we are left with a single largest term under the parentheses ($B|\boldsymbol{a}|u_0 \sim B^{1/2}$), and approximating the denominator to the lowest order $I_b \approx I_0$ we arrive at

$$H = \frac{1}{2}(U_0^2 + B^2u_0^2) + \frac{1}{2}\left(\boldsymbol{W} - \mathrm{i}\frac{B}{2}\mathcal{G}\boldsymbol{w}\right)^2 + \frac{1}{2}\boldsymbol{w}^{\mathrm{T}}\mathcal{V}\boldsymbol{w}. \tag{20}$$

Here we introduced double-size vectors composed of two $(N-1)$-vectors:

$$\boldsymbol{w} = \{\tilde{\boldsymbol{u}}, \tilde{\boldsymbol{v}}\}, \qquad \boldsymbol{W} = \{\tilde{\boldsymbol{U}}, \tilde{\boldsymbol{V}}\}, \tag{21}$$

and the corresponding $(2N-2) \times (2N-2)$ matrices—a symmetric potential matrix

$$\mathcal{V} = \begin{pmatrix} \tilde{\mathcal{A}} & \tilde{\mathcal{B}} \\ \tilde{\mathcal{B}}^{\mathrm{T}} & \tilde{\mathcal{D}} \end{pmatrix} \tag{22}$$

and a Hermitian rotation matrix

$$\mathcal{G} = \begin{pmatrix} 0 & -\mathrm{i}\tilde{\mathcal{I}} \\ \mathrm{i}\tilde{\mathcal{I}} & 0 \end{pmatrix}, \tag{23}$$

with $\tilde{\mathcal{I}}$ denoting the $(N-1) \times (N-1)$ unity matrix.

2.3. Riccati equation

We now proceed to the solution of the Schrödinger equation

$$(H - E)\Psi = 0, \tag{24}$$

with H given by equation (20). The breathing mode separates and its (unnormalized) wavefunction reads

$$\psi_0(u_0) = \mathrm{e}^{-Bu_0^2/2}. \tag{25}$$

The remaining modes are more difficult to treat due to effects of the potential anisotropy (the sensitivity to the substitution $\tilde{\boldsymbol{u}} \leftrightarrows \tilde{\boldsymbol{v}}$) discussed in appendix B on the basis of a single two-dimensional anisotropic oscillator. However, since the potential is parabolic we are enabled to look for the ground state wavefunction in the form of a Gaussian, i.e., an exponentiated quadratic form, and we write the wavefunction of all $2N - 2$ vibrational modes as

$$\psi = \exp\left(-\frac{B}{4}\boldsymbol{w}^{\mathrm{T}}\mathcal{X}\boldsymbol{w}\right), \tag{26}$$

with an unknown complex symmetric $(2N - 2) \times (2N - 2)$ matrix $\mathcal{X}$.

We substitute equation (26) into the Schrödinger equation and recall that

$$\boldsymbol{W} = -\mathrm{i}\frac{\partial}{\partial \boldsymbol{w}}. \tag{27}$$

Performing a straightforward calculation and equating the coefficients that multiply different powers of coordinates we obtain the following two equations:

$$E = \frac{B}{4}\operatorname{Tr}\mathcal{X}, \tag{28a}$$

$$\mathcal{X}^2 + \mathcal{G}\mathcal{X} - \mathcal{X}\mathcal{G} - \mathcal{I} - \frac{4}{B^2}\mathcal{V} = 0. \tag{28b}$$

The first of these equations is an expression for the energy, while the second one is a quadratic matrix equation (the Riccati equation [25]) whose solution allows one to obtain the unknown matrix $\mathcal{X}$.

2.4. Solution

Although equation (28*b*) includes a small parameter B^{-2} we cannot make direct use of it due to the degeneracy of the problem. Therefore, we have to solve this equation exactly.

In a standard approach [25], the solution of the Riccati equation is mapped onto the spectral problem of an auxiliary $(4N - 4) \times (4N - 4)$ supermatrix

$$\mathcal{M} = \begin{pmatrix} \mathcal{G} & -\mathcal{I} \\ -(4\mathcal{V}/B^2 + \mathcal{I}) & \mathcal{G} \end{pmatrix}, \tag{29}$$

composed of the coefficients of equation (28*b*). As shown in [26], a physical interpretation of such a procedure is possible and amounts to the transition from the Schrödinger equation to the dynamic Heisenberg equations.

Indeed, introducing two $(2N - 2) \times (2N - 2)$ matrices

$$\mathcal{U}_1 = -\mathcal{X} + \mathcal{G}, \tag{30a}$$

$$\mathcal{U}_2 = \mathcal{G}\mathcal{X} - 4\mathcal{V}/B^2 - \mathcal{I}, \tag{30b}$$

we cast the Riccati equation into a system of three equations:

$$\mathcal{X}\mathcal{U}_1 = \mathcal{U}_2, \tag{31a}$$

$$\mathcal{G}\mathcal{U}_1 - \mathcal{U}_2 = \mathcal{U}_1\mathcal{U}_1, \tag{31b}$$

$$-(4\mathcal{V}/B^2 + \mathcal{I})\mathcal{U}_1 + \mathcal{G}\mathcal{U}_2 = \mathcal{U}_2\mathcal{U}_1. \tag{31c}$$

The first one is readily solved

$$\mathcal{X} = \mathcal{U}_2\mathcal{U}_1^{-1}, \tag{32}$$

and transforms the remaining two into a matrix equation

$$\mathcal{M}\mathcal{U} = \mathcal{U}\mathcal{U}_1, \tag{33}$$

where we introduced a tall matrix:

$$\mathcal{U} = \begin{pmatrix} \mathcal{U}_1 \\ \mathcal{U}_2 \end{pmatrix}, \tag{34}$$

with the number of rows twice that of columns.

The equation obtained, (33), resembles an eigenvalue problem written in a matrix form:

$$\mathcal{M}\mathcal{U} = \mathcal{U}\mathcal{L}. \tag{35}$$

Here, the matrix $\mathcal{U}$ is made up of eigenvectors of $\mathcal{M}$ arranged columnwise, and $\mathcal{L}$ is a diagonal matrix of the corresponding eigenvalues. Note that the matrix $\mathcal{U}$ may be restricted to a subset of the eigenvectors, as is the case in equation (33) where the number of columns in $\mathcal{U}$ is one half of the number of rows. Correspondingly, the matrix $\mathcal{L}$ should also be a smaller matrix whose order is equal to the number of columns in $\mathcal{U}$.

Moreover, equation (35) possesses many solutions since this equation is invariant with respect to the transformation

$$\mathcal{U} \to \mathcal{U}\mathcal{K}, \qquad \mathcal{L} \to \mathcal{K}^{-1}\mathcal{L}\mathcal{K}, \tag{36}$$

with an arbitrary nondegenerate matrix $\mathcal{K}$.

Comparing equations (33) and (35) we see that the modified eigenvalue problem becomes equivalent to the Riccati problem if we are able to find a transformation $\mathcal{K}$ connecting

$$\mathcal{U}_1\mathcal{K} = \mathcal{K}^{-1}\mathcal{L}\mathcal{K}. \tag{37}$$

However, this step is inessential since the sought solution

$$\mathcal{X} = (\mathcal{U}_2\mathcal{K})(\mathcal{U}_1\mathcal{K})^{-1} = \mathcal{U}_2\mathcal{U}_1^{-1} \tag{38}$$

is invariant with respect to the above transformation.

Let us point out that due to the very simple structure of the supermatrix (29) there exists a relation

$$\mathcal{U}_2 = \mathcal{G}\mathcal{U}_1 - \mathcal{U}_1\mathcal{L}, \tag{39}$$

which allows us to write down the final solution to the Riccati equation in the form

$$\mathcal{X} = \mathcal{G} - \mathcal{U}_1\mathcal{L}\mathcal{U}_1^{-1}. \tag{40}$$

Employing the considerations outlined in [26] one may show that the eigenvalues of the matrix $\mathcal{M}$ come in pairs $\pm\lambda_n$ ($0 \leqslant n < 2N-2$). It follows then from equation (40) that we must pick all negative eigenvalues in order to obtain a positive definite $\mathcal{X}$ which ensures the correct behaviour of the wavefunction (26).

In summary, the Riccati equation (28*b*) is solved using the following steps: (i) a large auxiliary matrix $\mathcal{M}$ is set up, (ii) its eigenvalues and eigenvectors are found, and (iii) the negative part of the spectrum is used to compose $\mathcal{U}_1$ and $\mathcal{U}_2$. The final result is given by equation (40).

As a matter of fact, the above procedure is numerically unstable at magnetic fields $B \gg 1$ since in this limit the eigenvalues of $\mathcal{M}$ condense into nearly degenerate clusters located around 0 and ± 2 (while those of the original Schrödinger equation condense into the Landau

levels). Thus it is advisable to find the spectral information on $\mathcal{M}$ using a more stable Schur decomposition:

$$\mathcal{M}\mathcal{U} = \mathcal{U}\mathcal{S} \tag{41}$$

which resembles equation (35), except that the diagonal eigenvalue matrix $\mathcal{L}$ is replaced by an upper triangular Schur matrix $\mathcal{S}$ with the same eigenvalues on the diagonal.

We employed this procedure to obtain the results discussed in the following section. The numerical routine was built around several calls to the LAPACK numerical library [27].

3. Correlation functions

Equations (26) and (25) express the quasiclassical many-electron wavefunction as a function of the collective coordinates $\boldsymbol{u}$ and $\boldsymbol{v}$. We obtain the wavefunction in the $\boldsymbol{x}$ and $\boldsymbol{y}$ coordinates of the rotating frame employing the transformation $\mathcal{Q}^{\mathrm{T}}$, inverse to that applied in equations (8) and (11).

The transformation back to the laboratory coordinates $(\boldsymbol{\xi}, \boldsymbol{\eta})$ is accomplished by generalizing the procedure described in section 6 of [18]. Considering the modified versions of equations (31)–(36) of [18] we obtain

$$\boldsymbol{x} = \boldsymbol{\xi}, \tag{42a}$$

$$\boldsymbol{y} = (1 - \boldsymbol{Q}_0\boldsymbol{Q}_0^{\mathrm{T}})\boldsymbol{\eta}, \tag{42b}$$

with the vector $\boldsymbol{Q}_0$ defined in equation (9). Thus, the radial coordinates of the two frames coincide, while the azimuthal ones are connected by a projection operator which ensures the elimination of the rotation mode. Therefore, transformation of the vibrational wavefunction to the laboratory frame preserves the wavefunction form and only replaces the coordinates.

The knowledge of the wavefunction provides complete information on the distribution of charge and currents in a quantum dot. In the following discussion, we confine our attention to the distribution of charge since (as is shown in [18]) the distribution of charge also determines the distribution of currents. The electron charge density itself is of limited interest as this quantity retains the full symmetry of the Hamiltonian and hides the manifestation of the inter-particle correlation in the internal structure of a quantum dot. In order to reveal this structure, which is of primary interest to us, we calculate the density–density correlation function.

Generally, this function is interpreted as the conditional distribution of the charge density as a function of coordinate $\boldsymbol{r}$ given that one electron is pinned at a certain reference point $\boldsymbol{r}_0$. Restricting our consideration to the quasiclassical limit we can obtain this function in a rather simple way. The point is that in this regime the electrons become individualized by crystallizing into non-overlapping charge density lumps, each centred at the respective equilibrium position. Thus, the correlation function is only non-zero in the vicinity of one of the crystallization points and can be expressed as a sum of the partial contributions due to the individual electrons. Therefore, we evaluate the correlation function in the following manner:

(i) the coordinates of the pinned electron are set to zero as we always choose to fix the reference electron in its equilibrium position, and
(ii) the coordinates of all remaining electrons—except the one whose contribution we are interested in—are integrated over.

We perform the integration procedure numerically since the matrix of the quadratic form $\mathcal{X}$ as well as its transformation to the local coordinates are known only numerically. The integration over the kth variable is done by forming a complete square and can be formulated

as a transformation of the matrix $\mathcal{X}$: all matrix elements $\mathcal{X}_{ik}$ and $\mathcal{X}_{ki}$ are set to zero while the remaining entries transform according to

$$\mathcal{X}_{ij} \to \mathcal{X}_{ij} - \frac{\mathcal{X}_{ik}\mathcal{X}_{kj}}{\mathcal{X}_{kk}^2} \qquad i, j \neq k. \tag{43}$$

The result of a complete series of steps (43) is the partial contribution of one of the electrons to the total correlation function which we obtain in the form of a Gaussian function. Note that we are able to disregard the normalization of the wavefunction in the intermediate steps and only normalize the final result to unity. The constant density lines obtained from a Gaussian function are ellipses which we characterize by determining the ratio of the major and minor axes and their orientation with respect to the local x, y frames.

3.1. Single-ring quantum dots

When the number of electrons in a parabolic quantum dot is $2 \leqslant N \leqslant 5$, the electrons crystallize into a single ring with equilibrium positions arranged at equal intervals. In this case we are able to compare our results to those obtained from an earlier calculation [18] which, besides being limited to single-ring configurations, does not take the potential anisotropy into account.

For the simplest, two- and three-electron, quantum dots we obtain a quadratic form of the wavefunction identical to that given in equation (21*b*) of [18]. This agreement stems from the complete absence of anisotropy in the potential (22) which we also verified by an analytic calculation. As a consequence, in the correlation functions we find charge density ellipses elongated in the azimuthal direction with the ratios of axes

$$p_2 = \sqrt{3} \approx 1.732, \qquad p_3 = \sqrt{\tfrac{5}{2}} \approx 1.581, \tag{44}$$

for two- and three-electron quantum dots, respectively.

However, for quantum dots with four and five electrons we do find that the potential is anisotropic and the ratios of axes are

$$p_4 = \begin{cases} 1.402 \\ 1.444 \\ (1.528) \end{cases}, \qquad p_5 = \begin{cases} 1.218 \\ 1.263 \\ (1.5). \end{cases} \tag{45}$$

The two top lines in equation (45) correspond, respectively, to the electrons that neighbour the pinned one and the remote ones. The bottom line shows the result obtained from [18], which is the same for all electrons. The correlation functions are sketched in figure 1. Here, the full lines indicate the elliptic shapes of charge density lumps obtained from the present theory and are compared to the earlier proposed results drawn by the dotted lines. These plots are meant to indicate only the shape of the charge density lumps and not their absolute dimensions which scale as $B^{-1/2}$. We see that in the case of four-electron quantum dots, the effects due to the potential anisotropy turn out to be small and the difference between the two sets of lines is hardly discernible. On the other hand, for five-electron quantum dots (which were not considered in [18]), the disagreement is quite conspicuous.

Thus, we conclude that the proper account for the potential anisotropy makes two notable and reasonable changes. For one thing, the ratio p_N now indicates a general decreasing behaviour with increasing electron number N. This is very natural, since a greater number of electrons on the ring leaves less freedom for azimuthal motion. Moreover, now the electrons neighbouring the pinned one have less azimuthal freedom than the remote ones.

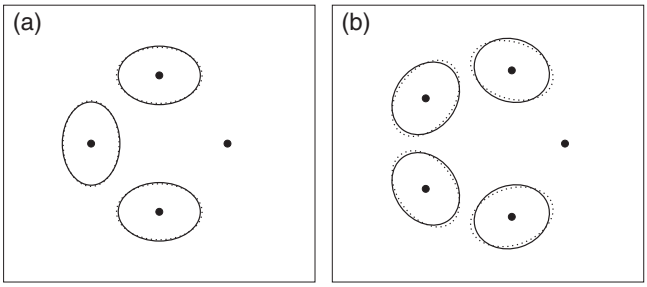

Figure 1. Correlation functions of four- (a) and five-electron (b) quantum dots. Full (dotted) lines indicate the shape of the charge density lumps with (without) inclusion of the potential anisotropy.

3.2. More than one electron ring

When the number of electrons in a parabolic quantum dot is $N = 6$ or higher the configuration in which a single ring accommodates all electrons is not the energetically preferred one, and a shell structure develops [19]. Being equipped with a computational scheme capable of treating general configurations, we shall now take a look at two-ring systems.

As a matter of fact, when the number of electrons is $6 \leqslant N \leqslant 8$ the inner shell consists of but one electron located in the minimum of the confining potential, and the remaining $N - 1$ electrons sit equidistantly on the outer ring. This configuration turns out to be quite similar to the single-ring structure.

Calculating the elongations of the charge density ellipses for this case we obtain

$$p_6 = \begin{cases} 1.611 \\ 1.735 \end{cases}, \qquad p_7 = \begin{cases} 1.400 \\ 1.493 \\ 1.522 \end{cases}, \qquad p_8 = \begin{cases} 1.208 \\ 1.276 \\ 1.309. \end{cases} \tag{46}$$

Here, as before, the top line belongs to the nearest neighbours of the pinned electron and the following lines to the second-and third-(if such exist) nearest neighbours. The charge density lump of the central electron has a nearly circular shape and we will not consider it in more detail. The results (46) follow the same trend as those of single-ring systems (equation (45)), thereby confirming the likeness of these two configurations.

A notable qualitative difference (albeit quantitatively small) is that the major axes of the ellipses in the present case do not always point in the azimuthal (y) direction. Generally, they are rotated by a small angle which does not exceed 2.5°.

For even greater number of electrons ($N \geqslant 9$), at least one well defined (that is, not reducing to a single point) inner ring is present. Among these systems, in nine- and ten-electron quantum dots the inner ring consists of a two-electron dumb-bell which in turn deforms the outer ring of electrons. Thus, the ground state configuration of these quantum dots is not circularly symmetric, and has an elliptic shape.

Let us consider the ten-electron quantum dot whose ground state configuration still retains a considerable degree of symmetry, namely, two perpendicular symmetry axes. However, as we will see shortly, the dynamical stability of this remaining symmetry of the ten-electron quantum dot is very weak.

Figure 2 shows the correlation functions obtained in two cases when an electron in either outer (panel (a)) or inner ring (panel (b)) is pinned. The situation in the outer ring resembles that found in simpler quantum dots—when one electron is pinned the charge densities of the remaining ones assume a slightly elongated elliptic shape. However, in the present case the

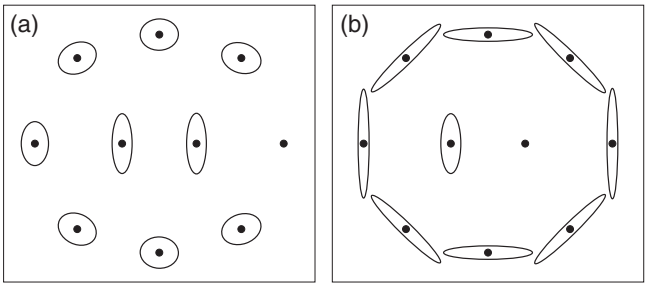

Figure 2. Correlation functions of a ten-electron dot. The conditional distribution of the charge density when an electron in the outer (a) or inner (b) ring is pinned.

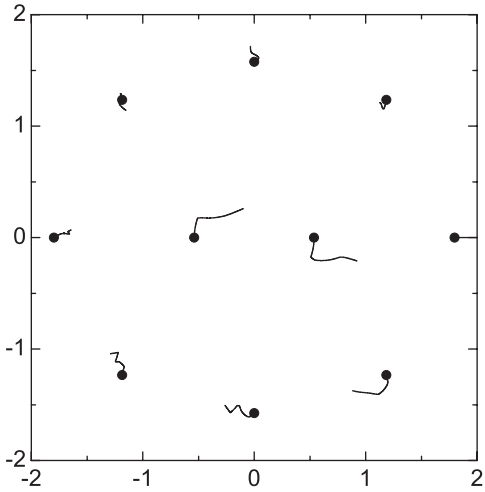

Figure 3. Monte Carlo trajectories of a ten-electron quantum dot. The dots mark the equilibrium positions of electrons.

major axes of the ellipses may deviate quite a lot (up to 24°) from the azimuthal direction. The inner shell electrons are relatively free to perform the azimuthal motion, and their charge density ellipses are characterized by ratios of axes around 3.

Likewise, when an electron of the inner shell is pinned, the ellipses of the outer ring charge density lumps are visibly elongated in the azimuthal direction with the ratio of axes reaching 10. This value corresponds to roughly the same angular extent as in the previous case of the response of the inner electrons to the pinning of an outer one.

These facts hint at the weakness of the angular correlation between the different shells and ease of the inter-shell rotation. Indeed, inspecting the eigenvalues of the potential matrix we find a very small eigenvalue $\lambda_1 = 1.5 \times 10^{-9}$, to be compared to the second lowest $\lambda_2 = 4 \times 10^{-3}$.

We would also like to point out that the above-discussed weak stability of the ten-electron quantum dot is already visible from the final snippets of the Monte Carlo trajectories shown in figure 3. While performing the simulation the most distant electron was kept on the positive part of the x axis by supplementing Monte Carlo steps with a rotation of the dot as a whole. We see that the two inner electrons first reach positions on the inner circle slightly off the x axis, and then slowly relax to the equilibrium positions on the x axis, whereas the remaining

electrons approach their equilibrium positions from more or less random directions. The energy change associated with this last leg of trajectories is only of the order of 10^{-6}, seven orders of magnitude below the total energy of this configuration ($E \approx 35.6$).

In conclusion, we developed a mathematical framework for calculation of the ground state of many-electron parabolic quantum dots in strong magnetic fields. Using this scheme we demonstrated that the anisotropy of the potential felt by the electrons influences the electron density even in the limit of infinite magnetic fields and therefore must be taken into account. The correlation functions show a substantial deformation of Wigner molecules and the possibility of soft modes related to the inter-shell rotation.

Appendix A. Symmetries of the parabolic dot

A parabolically confined quantum dot possesses a number of symmetries that significantly aid the solution of the many-electron problem. Among these are: (i) the separation of the centre of mass motion [2, 28], (ii) decoupling of the rotation of the system as a whole which takes places under much more general conditions of the isotropic confinement, and (iii) separation of the breathing mode [29, 30]. In this appendix, we present the calculation of the potential matrix needed in the main text which also provides an immediate proof of the above point (iii).

Since the Coulomb interaction is invariant with respect to rotations of the system as a whole, we use the potential (2) expansion in the laboratory frame. The equilibrium configuration is found by equating the first derivative to zero:

$$V_n = \nabla_n V|_{r_n=a_n} = \boldsymbol{a}_n - \lambda \sum_{\substack{m,n=1 \\ m\neq n}}^{N} \frac{\boldsymbol{a}_n - \boldsymbol{a}_m}{|\boldsymbol{a}_n - \boldsymbol{a}_m|^3} = 0, \tag{A.1}$$

and the second term—the potential matrix itself—reads

$$V_{nm} = (\nabla_n \otimes \nabla_m V)|_{r_n=a_n} = \delta_{nm} + [1-\delta_{nm}]\left\{ \frac{\lambda}{|\boldsymbol{a}_n - \boldsymbol{a}_m|^3} - 3\lambda \frac{(\boldsymbol{a}_n - \boldsymbol{a}_m)\otimes(\boldsymbol{a}_n - \boldsymbol{a}_m)}{|\boldsymbol{a}_n - \boldsymbol{a}_m|^5} \right\}$$
$$- \delta_{nm} \sum_{\substack{m,n=1 \\ m\neq n}}^{N} \left\{ \frac{\lambda}{|\boldsymbol{a}_n - \boldsymbol{a}_m|^3} - 3\lambda \frac{(\boldsymbol{a}_n - \boldsymbol{a}_m)\otimes(\boldsymbol{a}_n - \boldsymbol{a}_m)}{|\boldsymbol{a}_n - \boldsymbol{a}_m|^5} \right\}, \tag{A.2}$$

with the symbol $\otimes$ denoting the outer product of two vectors.

Multiplying the matrix element (A.2) by the vector $\boldsymbol{a}_m$, performing the summation over m and taking into account equation (A.1) we obtain

$$\sum_{m=1}^{N} V_{nm}\boldsymbol{a}_m = \boldsymbol{a}_n + 2\lambda \sum_{\substack{m,n=1 \\ m\neq n}}^{N} \frac{\boldsymbol{a}_n - \boldsymbol{a}_m}{|\boldsymbol{a}_n - \boldsymbol{a}_m|^3} = 3\boldsymbol{a}_n. \tag{A.3}$$

Thus we establish that the vector $\{\boldsymbol{a}_1, \boldsymbol{a}_2, \ldots, \boldsymbol{a}_N\}$ or the same vector written in the local frame

$$\boldsymbol{a} = \{a_1, a_2, \ldots, a_N\} \tag{A.4}$$

is an eigenvector of the potential matrix corresponding to the eigenvalue 3 for any number of electrons. That is, an electron system in a parabolic confinement has a separable universal breathing mode.

Appendix B. Electron in anisotropic parabolic potential

A general consideration of the problem of the anisotropic harmonic oscillator in a magnetic field is given in [31]. Here we provide a shortcut calculation of the ground state emphasizing the persistence of effects due to the potential anisotropy even in the limit of extreme magnetic fields.

We consider the Hamiltonian

$$H = -\frac{1}{2}\left[\left(\frac{\partial}{\partial x} - \mathrm{i}\frac{B}{2}y\right)^2 + \left(\frac{\partial}{\partial y} + \mathrm{i}\frac{B}{2}x\right)^2\right] + \frac{1}{2}(ax^2 + by^2), \tag{B.1}$$

and look for the ground state wavefunction of the form

$$\Psi(\boldsymbol{r}) = \exp\{-\tfrac{1}{2}(F_1x^2 + F_2y^2 + 2\mathrm{i}Gxy)\}. \tag{B.2}$$

Inserting (B.2) into the stationary Schrödinger equation $(H - E)\Psi(\boldsymbol{r}) = 0$ and collecting the coefficients of terms proportional to x^2, y^2, xy and 1 we generate the following set of coupled equations:

$$\begin{aligned} &-F_1^2 + (B/2 - G)^2 + a = 0,\\ &-F_2^2 + (B/2 + G)^2 + b = 0,\\ &F_1(B/2 + G) - F_2(B/2 - G) = 0,\\ &F_1 + F_2 - 2E = 0, \end{aligned} \tag{B.3}$$

for four unknowns: $F_{1\,(2)}$, G and E.

Solving the first two equations for $F_{1\,(2)}$, substituting the result into the third equation and simplifying we obtain

$$a(B/2 + G)^2 = b(B/2 - G)^2, \tag{B.4}$$

and express G in terms of the potential anharmonicity:

$$G = -B\delta, \qquad \delta = \frac{\sqrt{b} - \sqrt{a}}{\sqrt{b} + \sqrt{a}}. \tag{B.5}$$

With this result we finally arrive at the coefficients $F_{1\,(2)}$ which define the electron density:

$$F_{1\,(2)} = \left[B^2\left(\tfrac{1}{2} \pm \delta\right)^2 + a\right]^{1/2} \approx B\left(\tfrac{1}{2} \pm \delta\right). \tag{B.6}$$

We emphasize that the deformation is essential even in the extreme $B \to \infty$ case, which could be anticipated due to the degeneracy of the problem. In contrast, the influence of the symmetric part of the confining potential decays as $1/B$.

References

[1] Kouwenhoven L P, Austing D G and Tarucha S 2001 *Rep. Prog. Phys.* **64** 701
[2] Jacak L, Hawrylak P and Wójs A 1998 *Quantum Dots* (Berlin: Springer)
[3] Maksym P A, Imamura H, Mallon G P and Aoki H 2000 *J. Phys.: Condens. Matter* **12** R299
[4] Reimann S M and Manninen M 2002 *Rev. Mod. Phys.* **74** 1283
[5] Reimann S M, Koskinen M and Manninen M 2000 *Phys. Rev. Lett.* **62** 8108
[6] Yannouleas C and Landman U 2004 *Phys. Rev.* B **70** 235319
[7] Tavernier M B, Anisimovas E, Peeters F M, Szafran B, Adamowski J and Bednarek S 2003 *Phys. Rev.* B **68** 205305
[8] Mikhailov S A 2002 *Phys. Rev.* B **65** 115312
[9] Yang S R E and MacDonald A H 2002 *Phys. Rev.* B **66** 041304
[10] Kamilla R K and Jain J K 1995 *Phys. Rev.* B **52** 2798
[11] Jeon G S, Chang C C and Jain J K 2004 *J. Phys.: Condens. Matter* **16** L271

[12] Jeon G S, Chang C C and Jain J K 2004 *Phys. Rev.* B **69** 241304
[13] Jain J K 1989 *Phys. Rev. Lett.* **63** 199
[14] Jain J K 1990 *Phys. Rev.* B **41** 7653
[15] Yannouleas C and Landman U 2003 *Phys. Rev.* B **68** 035326
[16] Yannouleas C and Landman U 2002 *Phys. Rev.* B **66** 115315
[17] Anisimovas E, Matulis A, Tavernier M B and Peeters F M 2004 *Phys. Rev.* B **69** 075305
[18] Anisimovas E, Matulis A and Peeters F M 2004 *Phys. Rev.* B **70** 195334
[19] Bedanov V M and Peeters F M 1994 *Phys. Rev.* B **49** 2667
[20] Saint Jean M, Even C and Guthmann C 2001 *Europhys. Lett.* **55** 45
[21] Millo O, Katz D, Cao Y W and Banin U 2001 *Phys. Rev. Lett.* **86** 5751
[22] Maeda H and Gallagher T F 2004 *Phys. Rev. Lett.* **92** 133004
[23] Maksym P A 1996 *Phys. Rev.* B **53** 10871
[24] Eckart C 1935 *Phys. Rev.* **47** 552
[25] Abou-Kandil H, Freiling G, Ionescu V and Jank G 2003 *Matrix Riccati Equations in Control and Systems Theory* (Berlin: Springer)
[26] Pyragienė T and Matulis A 2000 *Physica* E **8** 230
[27] Anderson E, Bai Z, Bischof C, Blackford S, Demmel J, Dongarra J, Du Croz J, Greenbaum A, Hammarling S, McKenney A and Sorensen D 1999 *LAPACK Users' Guide* 3rd edn (Philadelphia, PA: SIAM)
[28] Hawrylak P 1993 *Phys. Rev. Lett.* **71** 3347
[29] Schweigert V A and Peeters F M 1995 *Phys. Rev.* B **51** 7700
[30] Geller M R and Vignale G 1996 *Phys. Rev.* B **53** 6979
[31] Dippel O, Schmelcher P and Cederbaum L S 1994 *Phys. Rev.* A **49** 4415